

The Impact of Mass and Length Variations on Chaos in the Double Pendulum System: A Numerical Study



Mohamed Abd El-Hamid, STEM High School for Boys – 6th of October

Abstract

In this study, we delved into the impact of mass and length variations on the chaotic behavior of the double pendulum (DP), a classic nonlinear dynamical system. While prior studies have examined the effect of initial conditions like amplitude and angular velocity on DP chaos, a more quantitative analysis of the critical system parameters, mass, and length is necessary. We addressed this gap through numerical simulations in MATLAB, generating eight distinct DP configurations by independently altering each pendulum arm's mass and length values relative to a control case. We analyzed phase portraits, Poincaré sections, bifurcation diagrams, Lyapunov exponents, and Hamiltonians for each simulation to characterize chaos. Our results demonstrated that increasing either mass or length amplifies chaotic motions, with the lower pendulum's properties playing the more decisive role. Specifically, a heavier and longer lower pendulum induced greater dynamical instability and unpredictability. These results can further enhance our understanding of chaos and support the development of real-life applications such as robotic arms or self-balancing vehicles by improving their stability, allowing for effective control strategies, and conducting sensitivity analyses in dynamical systems.

Keywords: Double pendulum, Chaos theory, Nonlinear systems, Dynamical systems, Poincaré section, Bifurcation diagram, Lyapunov exponent

I. Introduction

The double pendulum, also known as a chaos pendulum, is a simple physical system that exhibits rich, dynamic behavior with a strong sensitivity to initial conditions [1]. It is a system that comprises of another pendulum attached to its end, and its motion is governed by a set of coupled ordinary differential equations [2]. Despite its apparent simplicity, the double pendulum exhibits remarkably chaotic behavior and has the potential to yield valuable knowledge through investigation. Chaos is typical in nonlinear dynamical systems and is characterized by

its aperiodic behavior in a deterministic system that shows sensitive dependence on initial conditions. Understanding the chaotic behavior of such systems is vital for advancing our knowledge in various fields of science and engineering.

The behavior of the double pendulum is quite intriguing, as it shows periodic behavior at low energy, transforms to quasi-periodicity at intermediate energy level and chaos at a higher energy level, and finally again, periodic motion as the system's energy increases further [3].

Notably, much experimental and numerical research into the double pendulum has been conducted, focusing on changes in the initial values of variables such as amplitude or angular velocity. However, the dependence of such systems on mass and length has received much less attention, and we aim to address this gap with our work. Such a study is essential for controlling and optimizing dynamical systems based on DP, such as robotic arms or self-balancing scooters, resulting in more accurate and effective strategies capable of overcoming the chaos in such systems.

In this paper, we will derive the equations of motion for the double pendulum using Lagrangian mechanics, conduct a simulation in MATLAB, and analyze the findings. The results will be represented in Phase portrait, Poincare sections, bifurcation diagrams, and the Lyapunov characteristic exponent. The Lyapunov exponent often describes a dynamical system's chaos. For instance, the system is not chaotic if the average Lyapunov exponent value is negative. However, if the Lyapunov exponent is positive, chaos is evident.

Our research aims to advance our understanding of the complex connections between the double pendulum's mass, length, and chaotic behavior and the relationships driving unexpected natural phenomena. This study aims to unravel the secrets of chaos in the double pendulum and connect the theoretical foundation with practical applications, bringing us one step closer to a day when unpredictable systems may be anticipated with great precision and under our control.

II. Background Information

i. Pendulum

A single gravity pendulum is a body suspended from a fixed point, allowing it to swing back and forth while being pulled by gravity. When a pendulum is released from its equilibrium position, it experiences a restoring force that pulls it back towards the

equilibrium position. The pendulum converts its kinetic energy to gravitational potential energy and back again, with the time for one complete cycle known as the "Period." The period depends mainly on the pendulum's length [4].

The simple gravity pendulum is an idealized mathematical model of the pendulum [5]. In these ideal conditions, with no damping force, the pendulum will hypothetically swing forever according to the law of conservation of energy. For this study's MATLAB simulation, there will be no damping.

As shown in Figure 1, pendulums are divided into two main types: simple and physical. A simple pendulum assumes that all its mass is located at the furthest point from the pivot, making it ideal for calculations but impossible to recreate perfectly in real life. In this investigation, we will focus on a simple double pendulum.

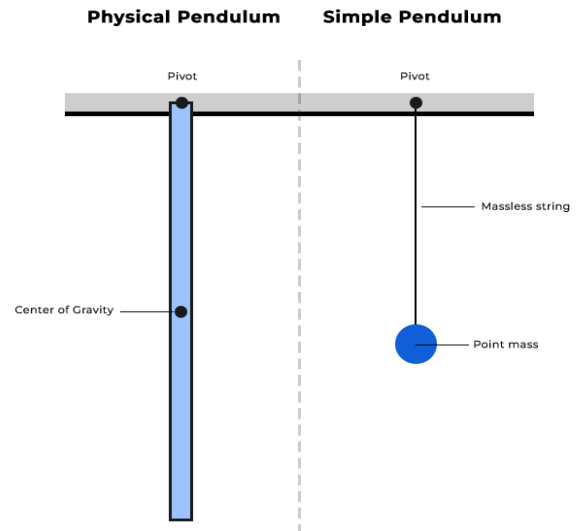


Figure 1: Comparison between physical pendulum and simple pendulum.

ii. Lagrangian Mechanics

Lagrangian mechanics is a widely used tool for analyzing double pendulums. To simulate the

motion of a double pendulum in MATLAB, we can use Lagrangian mechanics. Unlike traditional Newtonian mechanics, Lagrangian equations revolve around the principle of stationary action. This principle states that the path a system takes between two points in space and time is the one for which the step is stationary [6][7]. The benefit of using these equations is that they do not require considering the constraint between forces, such as the string's tension.

Instead of forces, Lagrangian mechanics uses the energies present in the system. The equations of motion are derived from the Euler-Lagrange equation, ensuring the action is minimized. Lagrangian mechanics describes a mechanical system as a pair (M, L) consisting of a configuration space M and a smooth function L within that space called a Lagrangian. The Lagrangian is a function that summarizes the dynamics of the entire system [8]. For many systems the Lagrangian is given as follows:

$$L = T - V \quad (1)$$

where T and V are the kinetic and potential energy of the system, respectively.

A central concept of Lagrangian mechanics is the action, which characterizes the trajectory of an object in space and time. The action is defined as an integral of the Lagrangian over time [9]. The following integral gives the action (A) of a specific trajectory:

$$A = \int_{t_1}^{t_2} L(T, V) dt \quad (2)$$

Physical systems tend to move in a specific path that minimizes the action, reflecting the principle of stationary action.

The equations of motion in Lagrangian mechanics are determined using the Euler-Lagrange equation. This fundamental rule describes the principle of stationary action. The Euler-Lagrange equation is given by:

$$\frac{d}{dt} \frac{\partial L}{\partial \dot{x}} = \frac{\partial L}{\partial x} \quad (3)$$

These equations describe the system's evolution over time and are fundamental to understanding the behavior of mechanical systems.

iii. Chaos Theory

Chaos theory is an interdisciplinary field of scientific research and a branch of mathematics that studies the underlying patterns and deterministic principles of dynamical systems. These systems were previously believed to have entirely random states of disorder and irregularity. Chaos theory explains how little modifications to one state of a deterministic nonlinear system may lead to significant variations in a subsequent state. This phenomenon is known as the butterfly effect. A double pendulum is an example of a chaotic system, showing significant sensitivity to initial conditions. [10][11][1]

To understand this phenomenon, it is crucial to quantify the chaos in a system. The Lyapunov exponent can be used to do so. The Lyapunov exponent is a quantity that characterizes the divergence of two trajectories with infinitely close initial conditions [12][13]. The magnitude of the divergence between the two trajectories at any point in time is represented as $\delta(t)$. $\delta(t)$ can be quantified as:

$$\delta(t) \approx \delta_0 e^{\lambda t} \psi \quad (4)$$

Here, δ is the Lyapunov exponent. A negative Lyapunov exponent would indicate that the points will eventually converge to a single value with increasing time. A positive Lyapunov exponent suggests that the points diverge from each other. Therefore, a positive Lyapunov exponent implies that the system is sensitive to its initial conditions and is hard to predict. Conversely, a negative Lyapunov exponent represents a non-chaotic system. [14]

III. Theory

As shown in Figure 2, the double pendulum is formed by two simple pendulums with lengths l_1 and l_2 , from which hang two spherical container masses: m_1 and m_2 . m_1 is the upper mass, and m_2 is the lower mass. At a certain time, the inextensible strings form angles θ_1 and θ_2 with respect to the vertical axis [15]. The upper end of the top pendulum is pivoted to a fixed point, while the lower end of the same pendulum is connected to the top end of the bottom pendulum [16].

In this simulation, the double pendulum is idealized to have no damping, and it is handled as a Hamiltonian system. Each pendulum is made up of a bob attached to a massless, rigid rod. The first pendulum's pivot is fixed at a point O . There is no friction in any action.

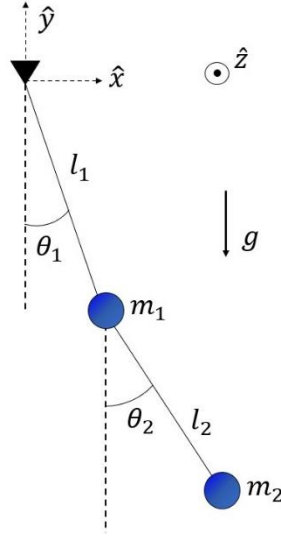


Figure 2: Diagram of the Double Pendulum

As shown in Figure 2, the positions of the bobs are given by:

$$x_1 = l_1 \sin \theta_1 \qquad y_1 = -l_1 \cos \theta_1 \qquad (5)$$

$$x_2 = l_1 \sin \theta_1 + l_2 \sin \theta_2 \qquad y_2 = -l_1 \cos \theta_1 - l_2 \cos \theta_2 \qquad (6)$$

To obtain the velocity of the bobs, we differentiate the above quantities with respect to time:

$$\dot{x}_1 = l_1 \dot{\theta}_1 \cos \theta_1 \qquad \dot{y}_1 = l_1 \dot{\theta}_1 \sin \theta_1 \qquad (7)$$

$$\dot{x}_2 = l_1 \dot{\theta}_1 \cos \theta_1 + l_2 \dot{\theta}_2 \cos \theta_2 \qquad \dot{y}_2 = l_1 \dot{\theta}_1 \sin \theta_1 + l_2 \dot{\theta}_2 \sin \theta_2 \qquad (8)$$

The Lagrangian for an undamped double pendulum free to move in place is given by:

$$L = T - V \qquad (9)$$

Using the expressions in Equations 7 and 8, the kinetic energy is:

$$\begin{aligned}
T &= \frac{1}{2}m_1v_1^2 + \frac{1}{2}m_2v_2^2 = \frac{1}{2}m_1(\dot{x}_1^2 + \dot{y}_1^2) + \frac{1}{2}m_2(\dot{x}_2^2 + \dot{y}_2^2) \\
&= \frac{1}{2}m_1l_1^2\dot{\theta}_1^2 + \frac{1}{2}m_2[l_1^2\dot{\theta}_1^2 + l_2^2\dot{\theta}_2^2 + 2l_1l_2\dot{\theta}_1\dot{\theta}_2 \cos(\theta_1 - \theta_2)]
\end{aligned} \tag{10}$$

The potential energy is the gravitational potential energy:

$$\begin{aligned}
V &= m_1gy_1 + m_2gy_2 = -m_1gl_1 \cos \theta_1 - m_2g(l_1 \cos \theta_1 + l_2 \cos \theta_2) \\
&= -(m_1 + m_2)gl_1 \cos \theta_1 - m_2gl_2 \cos \theta_2
\end{aligned} \tag{11}$$

The Lagrangian of the system is then:

$$L = \frac{1}{2}(m_1 + m_2)l_1^2\dot{\theta}_1^2 + \frac{1}{2}m_2l_2^2\dot{\theta}_2^2 + m_2l_1l_2\dot{\theta}_1\dot{\theta}_2 \cos(\theta_1 - \theta_2) + (m_1 + m_2)gl_1 \cos \theta_1 + m_2gl_2 \cos \theta_2 \tag{12}$$

The canonical momenta associated with the coordinates θ_1 and θ_2 can be obtained directly from L

$$p_{\theta_1} = \frac{\partial L}{\partial \dot{\theta}_1} = (m_1 + m_2)l_1^2\dot{\theta}_1 + m_2l_1l_2\dot{\theta}_2 \cos(\theta_1 - \theta_2) \tag{13}$$

$$p_{\theta_2} = \frac{\partial L}{\partial \dot{\theta}_2} = m_2l_2^2\dot{\theta}_2 + m_2l_1l_2\dot{\theta}_1 \cos(\theta_1 - \theta_2) \tag{14}$$

The equations of motion of the system are the Euler-Lagrange equations:

$$\frac{d}{dt} \left(\frac{\partial L}{\partial \dot{\theta}_i} \right) - \frac{\partial L}{\partial \theta_i} = 0 \Rightarrow \frac{dp_{\theta_i}}{dt} - \frac{\partial L}{\partial \theta_i} = 0 \quad \text{for } i = 1, 2 \tag{15}$$

Since:

$$\frac{dp_{\theta_1}}{dt} = (m_1 + m_2)l_1^2\ddot{\theta}_1 + m_2l_1l_2\ddot{\theta}_2 \cos(\theta_1 - \theta_2) - m_2l_1l_2\dot{\theta}_2\dot{\theta}_1 \sin(\theta_1 - \theta_2) + m_2l_1l_2\dot{\theta}_2^2 \sin(\theta_1 - \theta_2) \tag{16}$$

$$\frac{dp_{\theta_2}}{dt} = m_2l_2^2\ddot{\theta}_2 + m_2l_1l_2\ddot{\theta}_1 \cos(\theta_1 - \theta_2) - m_2l_1l_2\dot{\theta}_1^2 \sin(\theta_1 - \theta_2) + m_2l_1l_2\dot{\theta}_1\dot{\theta}_2 \sin(\theta_1 - \theta_2) \tag{16}$$

$$\frac{\partial L}{\partial \theta_1} = -m_2l_1l_2\dot{\theta}_1\dot{\theta}_2 \sin(\theta_1 - \theta_2) - (m_1 + m_2)gl_1 \sin \theta_1 \tag{18}$$

$$\frac{\partial L}{\partial \theta_2} = m_2l_1l_2\dot{\theta}_1\dot{\theta}_2 \sin(\theta_1 - \theta_2) - m_2gl_2 \sin \theta_2 \tag{19}$$

The equation simplifies to:

$$(m_1 + m_2)l_1\ddot{\theta}_1 + m_2l_2\ddot{\theta}_2 \cos(\theta_1 - \theta_2) + m_2l_2\dot{\theta}_2^2 \sin(\theta_1 - \theta_2) + (m_1 + m_2)g \sin \theta_1 = 0 \tag{20}$$

$$l_2\ddot{\theta}_2 + l_1\ddot{\theta}_1 \cos(\theta_1 - \theta_2) - l_1\dot{\theta}_1^2 \sin(\theta_1 - \theta_2) + g \sin \theta_2 = 0 \tag{21}$$

Simplifying and solving for θ :

$$\ddot{\theta}_1 = \frac{-m_2 l_2 \ddot{\theta}_2 \cos(\theta_1 - \theta_2) - m_2 l_2 \dot{\theta}_2^2 \sin(\theta_1 - \theta_2) - g(m_1 + m_2) \sin(\theta_1)}{(m_1 + m_2) l_1} \quad (22)$$

$$\ddot{\theta}_2 = \frac{-m_2 l_2 \ddot{\theta}_1 \cos(\theta_1 - \theta_2) + m_2 l_1 \dot{\theta}_1^2 \sin(\theta_1 - \theta_2) - m_2 g \sin(\theta_2)}{m_2 l_2} \quad (23)$$

Finally, equations 22 and 23 were solved numerically using MATLAB with the ode45 solver.

IV. Simulation and Experimental Setup

There are two ways to solve the equations of motion: either use a simulation based on a numerical approach or integrate the equations of motion to get an analytical solution [17]. We chose the latter and used MATLAB and integration techniques, specifically Runge-Kutta method, due to its precision and stability in capturing the system's behavior over time [18].

For all simulations, we maintained a constant set of initial conditions for angles and angular velocities, which were $(\theta_1, p_1, \theta_2, p_2) = (0.52, 0, 0.79, 0)$. Afterward, we conducted an extensive experiment to determine how mass (m_1 and m_2) and length (l_1 and l_2) influence the chaotic behavior of the DP. This involved two simulations for each variable, while keeping the others constant. The table below summarizes these scenarios.

Table 1: Simulation Scenarios for Mass and Length Variations

Case	M1 (Kg)	M2 (Kg)	L1 (m)	L2 (m)
Control	1	1	1	1
Case 1	2.5	1	1	1
Case 2	5	1	1	1
Case 3	1	2.5	1	1
Case 4	1	5	1	1
Case 5	1	1	2	1
Case 6	1	1	3	1
Case 7	1	1	1	2
Case 8	1	1	1	3

The simulation results consist of a phase portrait, bifurcation diagram, Poincare map. These visual representations offer a comprehensive understanding of the system's behavior [19] [20]. Moreover, the Lyapunov exponent is calculated to provide valuable insights into the system's chaotic behavior, which is a crucial component of Chaos theory [13] [21]. The simulation runs for 50 seconds, using 10000 timesteps of 0.005 seconds.

To ensure the accuracy and reliability of our simulations, we conducted a comparison analysis by aligning our outcomes with established literature wherever applicable.

V. Results and Discussion

Table 2: Lyapunov Exponents, Hamiltonians, and System Natures in Each Case

Case	Lyapunov Exponent	Hamiltonian	Nature
Control	-0.1082	-22.3430	Periodic
Case 1	-0.0486	-32.7714	Quasi-Periodic
Case 2	0.1248	-50.1488	Chaotic
Case 3	0.2682	-45.0665	Chaotic
Case 4	0.1028	-83.8674	Chaotic
Case 5	-0.0948	-36.1786	Quasi-periodic
Case 6	0.1025	-50.0282	Chaotic
Case 7	0.2256	-30.8818	Chaotic
Case 8	0.2536	-39.3719	Chaotic

i. Control Case (Figure 3)

As shown in Figure 3, the Lyapunov exponent of the control case is -0.1082 , indicating periodic motion. This periodicity provides valuable insights into the system's stability, highlighting the presence of recurrent patterns in its motion. The in-phase phase portrait shows that the motion is periodic, and the bifurcation diagram illustrates that the angular velocity is consistent with the forcing amplitude. Overall, these results indicate that the system is stable and behaves predictably.

$$e = -0.1082 \quad | \quad E = -22.3430 \text{ J}$$

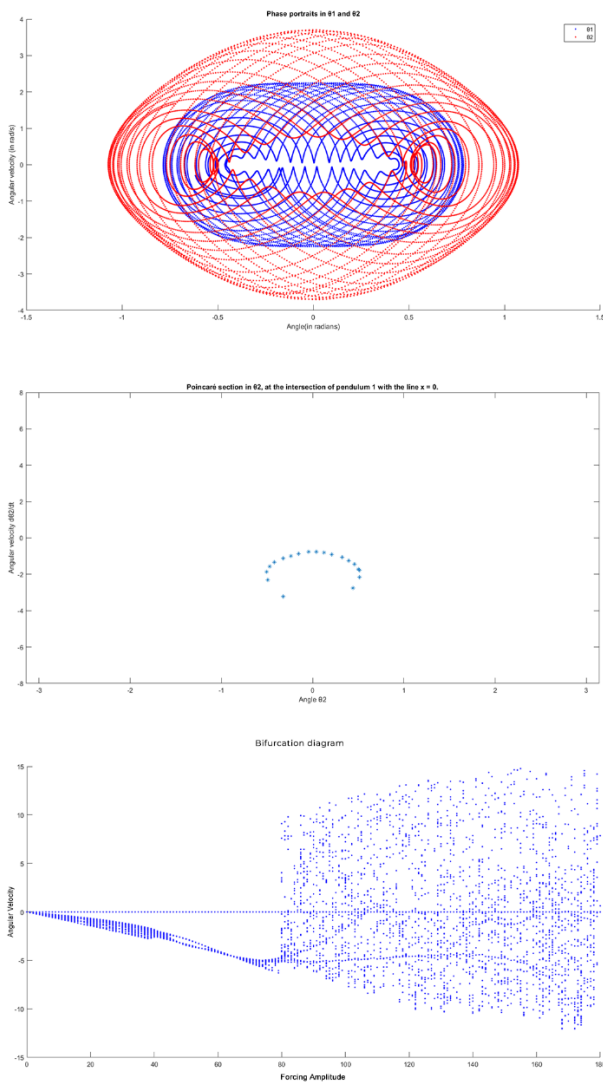


Figure 3: Control case results - Phase Portrait, Poincaré Section, and Bifurcation Diagram

ii. Case 1 (Figure 4)

Based on the observations made in Figure 4, with m_1 becoming 2.5 kg , the motion becomes less periodic in case 1, but it is still not chaotic. The phase portrait shows a quasi-phase relationship with a recognizable pattern, suggesting a certain degree of regularity within the system dynamics. Moreover, the Lyapunov exponent is -0.0486 , which is larger than the control case, meaning that the pendulum has a tendency to exhibit chaotic behavior but is still periodic due to its negative value. Additionally, the bifurcation diagram, when compared to the control case, displays no significant deviation, highlighting the system's stability despite the decreasing periodicity.

$$e = -0.0486 \quad | \quad E = -32.7714 \text{ J}$$

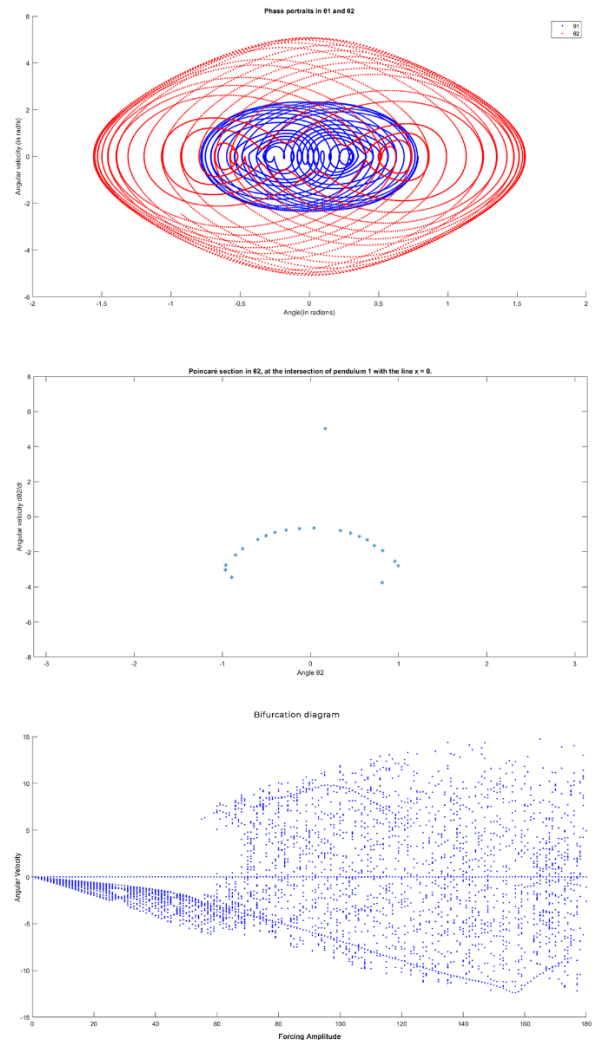


Figure 4: Case 1 results - Phase Portrait, Poincaré Section, and Bifurcation Diagram

iii. Case 2 (Figure 5)

According to Figure 5, as m_1 increased to 5 Kg, the pendulum's behavior became significantly more chaotic. The Lyapunov exponent of 0.1248 is notably higher than in the control and first case. The Poincaré map is dispersed, lacking a fixed area, indicating a high level of chaos. Additionally, the bifurcation diagram highly deviates from the control and first case.

$$e=0.1248 \quad | \quad E=-50.1488 \text{ J}$$

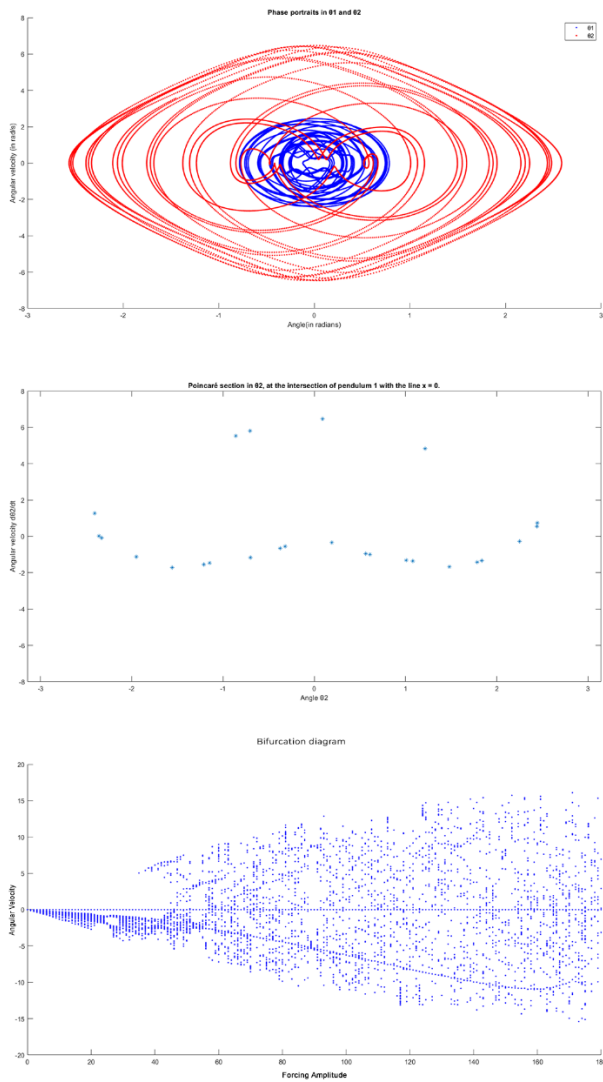


Figure 5: Case 2 results - Phase Portrait, Poincaré Section, and Bifurcation Diagram

iv. Case 3 (Figure 6)

In the third case, the mass of m_2 increased to 2.5 Kg. As shown in Figure 6, the phase portrait indicates a high degree of chaos compared to the control case. Additionally, the Poincaré section displays points that appear to be randomly scattered. The Lyapunov exponent, measuring 0.2682, is significantly higher than in cases 1 and 2, suggesting that chaos is more likely to occur with a lower mass (m_2) than with a higher mass (m_1). All of these factors contribute to the chaotic motion of the DP in case 3.

$$e=0.2682 \quad | \quad E=-45.0665 \text{ J}$$

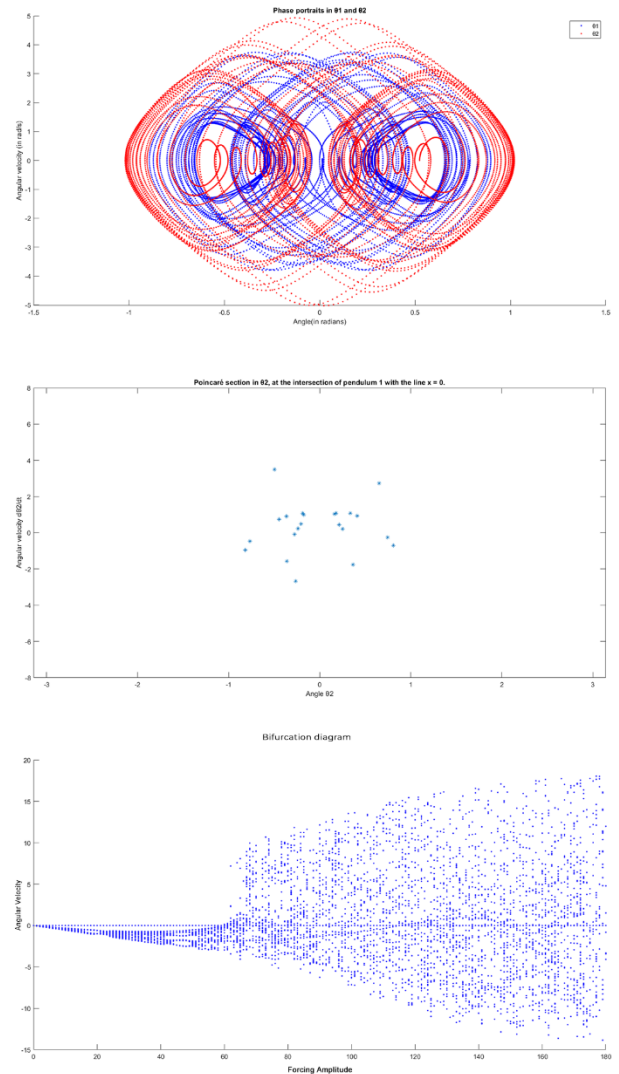


Figure 6: Case 3 results - Phase Portrait, Poincaré Section, and Bifurcation Diagram

v. Case 4 (Figure 7)

For case 4, according to Figure 7, the Lyapunov exponent decreased slightly compared to case 3 when m_2 was increased to 5 Kg, measuring at 0.1028. The Hamiltonian reached the highest value at -83.8674 J. Additionally, the Poincare section exhibited periodicity once more, with points clustering closely together. These findings support the initial hypothesis that the DP's motion tends to become periodic again at higher energy levels.

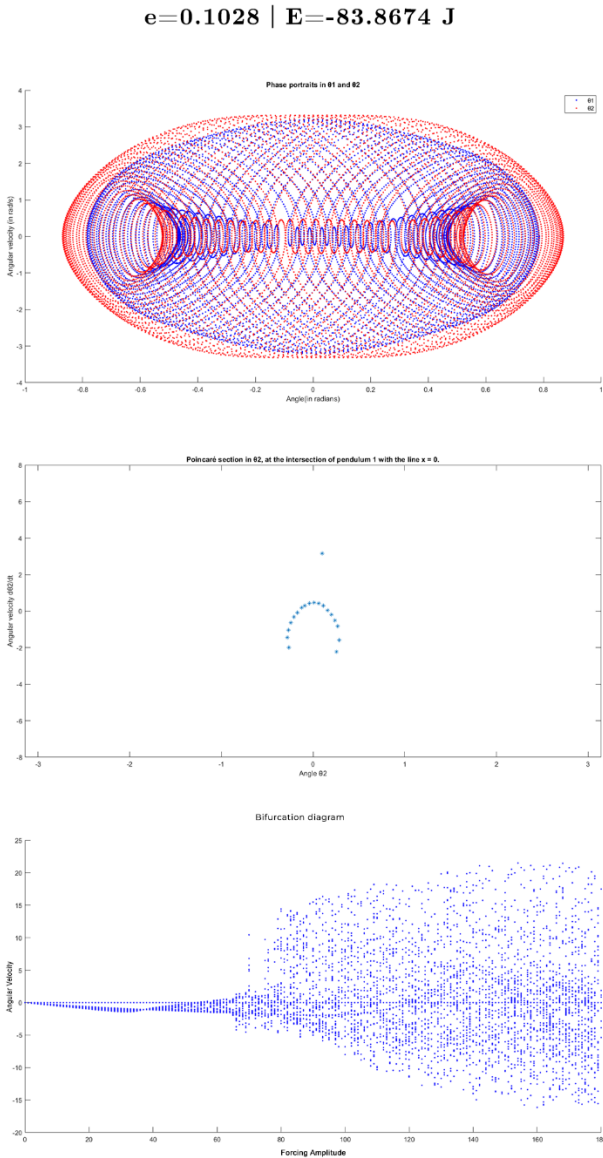


Figure 7: Case 4 results - Phase Portrait, Poincaré Section, and Bifurcation Diagram

vi. Case 5 (Figure 8)

In Figure 8, it can be observed that the phase portrait of case 5 showcases a distinct quasi-periodic pattern when the upper length (l_1) is increased to 2 m. Furthermore, the Poincare section reveals periodicity, while the Lyapunov exponent records at -0.0948, surpassing the control case, albeit remaining negative. These findings indicate that the motion is, in fact, quasi-periodic.

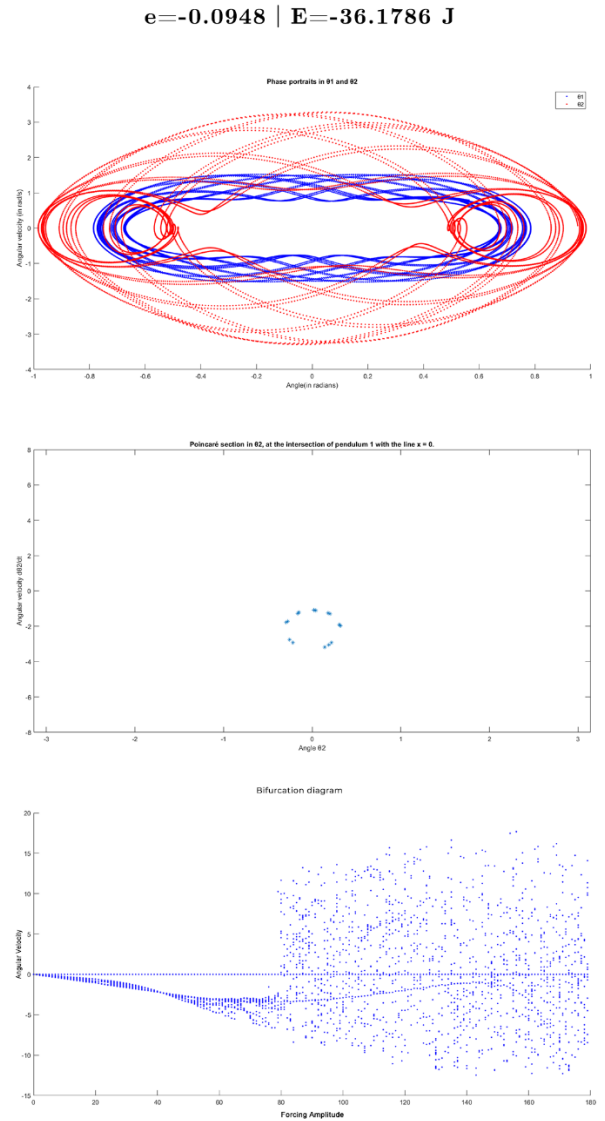


Figure 8: Case 5 results - Phase Portrait, Poincaré Section, and Bifurcation Diagram

vii. Case 6 (Figure 9)

The findings presented in figure 9's phase portrait and Poincaré section indicate that the double pendulum's movement becomes chaotic as the upper length increases to 5 m. This conclusion is reinforced by the positive Lyapunov exponent of 0.1025. Therefore, it can be deduced that the pendulum's upper length increase results in an escalated level of chaos.

$e=0.1025 \mid E=-50.0282 \text{ J}$

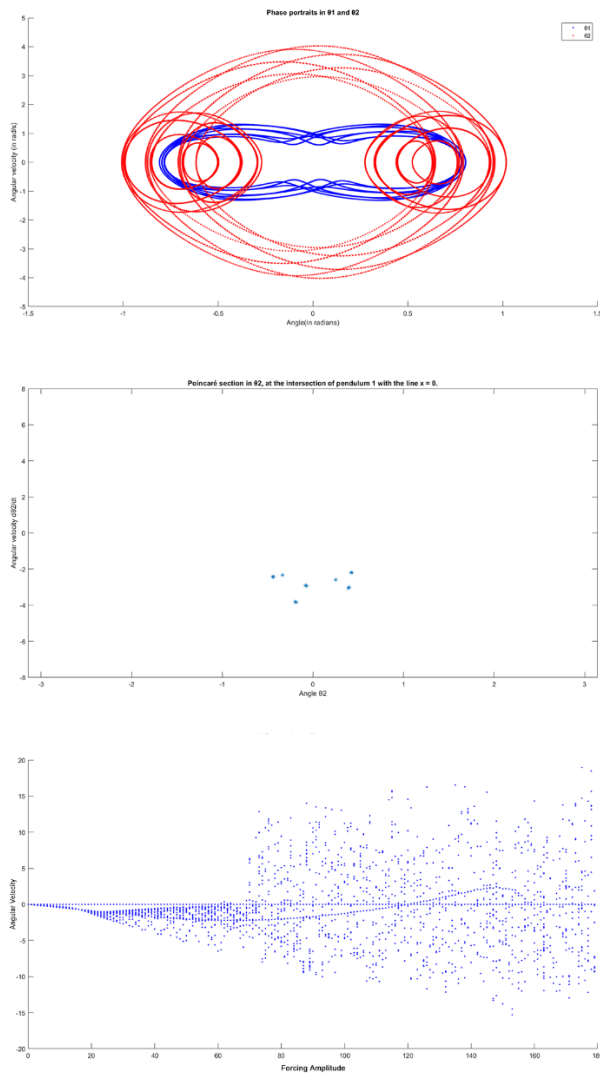


Figure 9: Case 6 results - Phase Portrait, Poincaré Section, and Bifurcation Diagram

viii. Case 7 (Figure 10)

Based on the insights presented in figure 10, when the lower length (l_2) of case 7 is extended to 2 m, the phase portrait and Poincaré section show chaos with a positive Lyapunov exponent of 0.2256. This value surpasses the results obtained from cases 5 and 6, where the upper length (l_1) was extended instead. These findings imply that augmenting the lower length (l_2) of the DP has a more significant effect on its chaotic dynamics than increasing the upper length.

$e=0.2256 \mid E=-30.8818 \text{ J}$

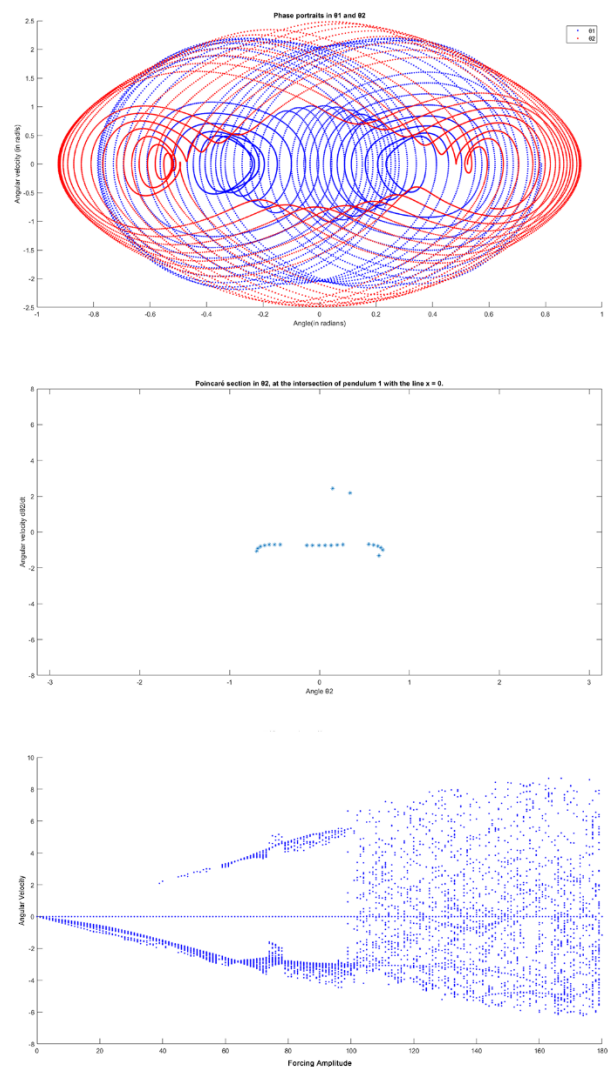


Figure 10: Case 7 results - Phase Portrait, Poincaré Section, and Bifurcation Diagram

ix. Case 8 (Figure 11)

In Figure 11, it is observed that case 8 exhibits a greater degree of chaos than case 7, with a Lyapunov exponent of 0.2536. This suggests that as the lower length increases, the level of chaos intensifies, as evidenced by the discrepancy between the Lyapunov exponent of the control case, case 7, and case 8.

$$e=0.2536 \mid E=-39.3719 \text{ J}$$

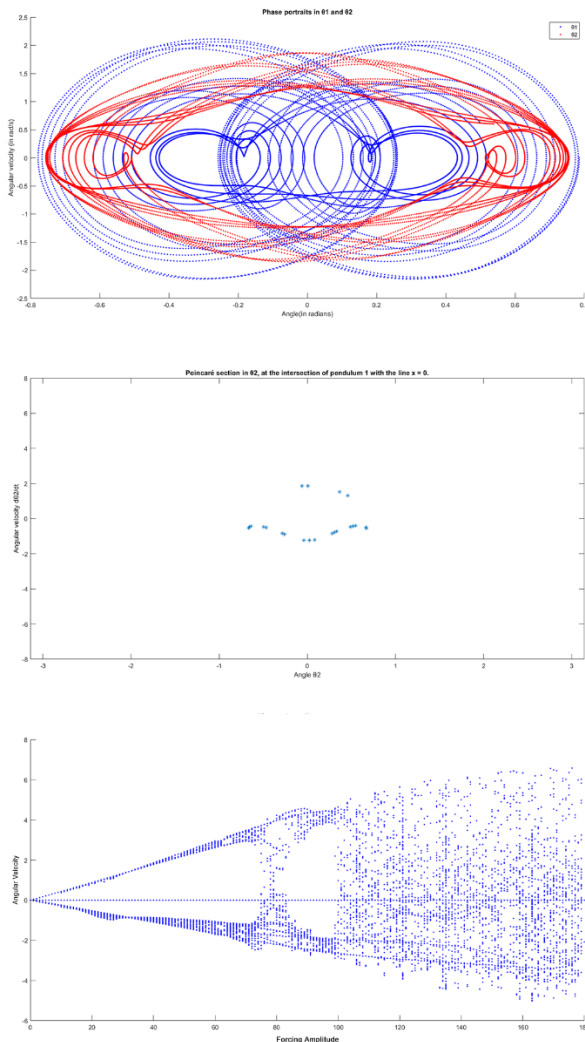


Figure 11: Case 8 results - Phase Portrait, Poincaré Section, and Bifurcation Diagram

VI. Conclusion

Studying the double pendulum is important due to its chaotic nature, and particularly its dependence on mass and length. In this paper, we conducted 9 simulations to test the relationship between upper and lower mass, as well as upper and lower length, on the chaotic behavior of the double pendulum. We presented the results in Poincaré sections, phase portraits, bifurcation diagrams, Lyapunov exponents, and Hamiltonians (energy). Our analysis shows that the chaotic behavior of the double pendulum increases with an increase in both mass and length, with the lower mass and length having a more significant effect on chaos than the upper ones. This study offers valuable insights into the behavior of the DP and can contribute to developing more accurate models and simulations in the future.

VII. References

[1] T. Shinbrot, C. Grebogi, J. Wisdom, and J. A. Yorke, "Chaos in a double pendulum," *American Journal of Physics*, vol. 60, no. 6, pp. 491–499, Jun. 1992. [Online]. Available:

<https://pubs.aip.org/ajp/article/60/6/491/1039046/Chaos-in-a-double-pendulum>

[2] R. B. Levien and S. M. Tan, "Double pendulum: An experiment in chaos," *American Journal of Physics*, vol. 61, no. 11, pp. 1038–1044, Nov. 1993. [Online]. Available:

<https://pubs.aip.org/ajp/article/61/11/1038/1054221/Double-pendulum-An-experiment-in-chaos>

[3] T. Stachowiak and T. Okada, "A numerical analysis of chaos in the double pendulum," *Chaos, Solitons & Fractals*, vol. 29, no. 2, pp. 417–422, Jul. 2006. [Online]. Available:

<https://linkinghub.elsevier.com/retrieve/pii/S0960077905006703>

[4] R. A. Nelson and M. G. Olsson, "The pendulum—Rich physics from a simple system," *American Journal of Physics*, vol. 54, no. 2, pp. 112–121, Feb. 1986. [Online]. Available:

<https://pubs.aip.org/ajp/article/54/2/112/1052629/The-pendulum-Rich-physics-from-a-simple-system>

[5] A. Ohlhoff and P. Richter, "Forces in the Double Pendulum," *ZAMM - Journal of Applied Mathematics and Mechanics / Zeitschrift für Angewandte Mathematik und Mechanik*, vol. 80, no. 8, pp. 517–534, 2000, eprint:

<https://onlinelibrary.wiley.com/doi/pdf/10.1002/1521-4001%28200008%2980%3A8%3C517%3A%3AID-ZAMM517%3E3.0.CO%3B2-1>.

[6] G. Layek, *An Introduction to Dynamical Systems and Chaos*. New Delhi: Springer India, 2015. [Online]. Available:

<http://link.springer.com/10.1007/978-81-322-2556-0>

[7] D. J. Acheson, *From calculus to chaos: an introduction to dynamics*. Oxford New York: Oxford university press, 1997.

[8] H. Biswas, M. M. Hasan, and S. Bala, "CHAOS THEORY AND ITS APPLICATIONS IN OUR REAL LIFE," *Barishal University Journal*, 2018.

[9] J. Heyl, "The Double Pendulum Fractal," *University of British Columbia Press*, 2008.

[10] S. Boccaletti, "The control of chaos: theory and applications," *Physics Reports*, vol. 329, no. 3, pp. 103–197, May 2000. [Online]. Available: <https://linkinghub.elsevier.com/retrieve/pii/S0370157399000964>

[11] G. P. Williams, *Chaos theory tamed*, reprod. Washington, DC: Henry, 1999

[12] H. J. Korsch, H.-J. Jodl, and T. Hartmann, *Chaos: A Program Collection for the PC*. Berlin, Heidelberg: Springer Berlin Heidelberg, 2008. [Online]. Available:

<https://link.springer.com/10.1007/978-3-540-74867-0>

[13] J. Ting and D. B. Marghitu, "Analyzing Double Pendulum Dynamics with Approximate Entropy and Maximal Lyapunov Exponent," in *Proceedings of the International Conference on Mechanical Engineering (ICOME 2022)*, I. Dumitru, L. Matei, L. D. Racila, and A. S. Rosca, Eds. Dordrecht: Atlantis Press International BV, 2023, vol. 15, pp. 167–174, series Title: Atlantis Highlights in Engineering. [Online]. Available:

https://www.atlantis-press.com/doi/10.2991/978-94-6463-152-4_19

[14] M. K. Gupta, K. Bansal, and A. K. Singh, "Mass and Length Dependent Chaotic Behavior of a Double Pendulum," *IFAC Proceedings Volumes*, vol. 47, no. 1, pp. 297–301, 2014. [Online]. Available: <https://linkinghub.elsevier.com/retrieve/pii/S1474667016326714>

[15] H. R. Dullin, "Melnikov's method applied to the double pendulum," *Zeitschrift für Physik B*

Condensed Matter, vol. 93, no. 4, pp. 521–528, Dec. 1994. [Online]. Available:

<http://link.springer.com/10.1007/BF01314257>

[16] M. Rafat, M. Hasan, and T. Wheatland, “Dynamics of a double pendulum with distributed mass,” American Journal of Physics, 2008.

[17] R. Mar, A. Goyal, V. Nguyen, T. Yang, and W. Singhose, “Combined input shaping and feedback control for double-pendulum systems,” Mechanical Systems and Signal Processing, vol. 85, pp. 267–277, Feb. 2017. [Online]. Available:

<https://linkinghub.elsevier.com/retrieve/pii/S0888327016302928>

[18] P. Schuster and H. Haken, Eds., Stochastic Phenomena and Chaotic Behaviour in Complex Systems, ser. Springer Series in Synergetics. Berlin, Heidelberg: Springer Berlin Heidelberg, 1984, vol. 21. [Online]. Available:

<http://link.springer.com/10.1007/978-3-642-69591-9>

[19] P. Yu and Q. Bi, “ANALYSIS OF NON-LINEAR DYNAMICS AND BIFURCATIONS OF A DOUBLE PENDULUM,” Journal of Sound and Vibration, vol. 217, no. 4, pp. 691–736, Nov. 1998. [Online]. Available:

<https://linkinghub.elsevier.com/retrieve/pii/S0022460X98917813>

[20] J. J. Bramburger and J. N. Kutz, “Poincaré maps for multiscale physics discovery and nonlinear Floquet theory,” Physica D: Nonlinear Phenomena, vol. 408, p. 132479, Jul. 2020. [Online]. Available:

<https://linkinghub.elsevier.com/retrieve/pii/S0167278919305470>

[21] J. B. Dingwell, “Lyapunov exponents,” Wiley encyclopedia of biomedical engineering, 2006.

VIII. Key Symbols

Symbol	Description
m_1, m_2	Masses of the upper and lower pendulum bobs, respectively (in kg).
l_1, l_2	Lengths of the upper and lower pendulums, respectively (in meters).
g	Acceleration due to gravity (in m/s^2).
x_1, y_1, x_2, y_2	Cartesian coordinates of the pendulum bobs in a two-dimensional plane (in meters).
$\dot{x}_1, \dot{y}_1, \dot{x}_2, \dot{y}_2$	Velocities of the pendulum bobs in the horizontal and vertical directions (in m/s).
θ_1, θ_2	Angles of the upper and lower pendulums (in radians) with respect to the vertical axis.
$\dot{\theta}_1, \dot{\theta}_2$	Angular velocities of the upper and lower pendulums (in rad/s).
$\ddot{\theta}_1, \ddot{\theta}_2$	Angular accelerations of the upper and lower pendulums (in rad/s^2).
$p_{\theta 1}, p_{\theta 2}$	Canonical momenta corresponding to θ_1 and θ_2 (in $\text{Kg} \cdot \text{m/s}$).
V	Potential energy of the system (in joules).
T	Kinetic energy of the system (in joules).
L	Lagrangian of the system (in joules).
H	Hamiltonian of the system, representing the total energy (in joules).
λ	Lyapunov exponent, a quantity that can detect the presence of chaos and quantify the stability or instability of the system (dimensionless).
A	Action (in $\text{Kg} \cdot \text{m}^2 \cdot \text{s}^{-1}$)
∂	Partial derivative symbol used in calculus to denote partial differentiation.